World Applied Sciences Journal 2 (3): 212-228, 2007
ISSN 1818-4952

Characterizing Land Cover Types and Surface Condition of Yardang Region in Lut Desert (Iran) Based upon Landsat Satellite Images

[1]S.K. Alavi Panah, [2]Ch. B. Komaki, [3]A. Goorabi and [4]H.R. Matinfar

[1]University of Tehran, P.O. Box: 14185-354, Iran
[2]Senior Expert of Desert Zone Management, Iran
[3]Department of Geomorphology, Faculty of Geography, University of Tehran
[4]University of Lorestan, Iran

Abstract: Lut Desert with an area of about 80,000 Km^2 has a great diversity of hydro-Aeolian processes with a very interesting pattern of yardang landforms. Although the yardang landscape in the Lut Desert is a good example of the wind and water erosion forms, but due to its poor accessibility, not so many researches was performed on it. To improve our understanding about one of the most interesting desert landforms, southeast of Lut Desert was selected. In this study, seven bands of Landsat Thematic Mapper (TM) data and some other sources of information includes topographic maps (1:50,000), aerial photos (1:20,000) plus fieldwork were used. The methodology comprised of; 1) Image processing 2) Fieldwork 3) Photo Morphic Unit Analysis (PMU) 4) Feature space analysis and 5) Image classification and accuracy assessment based on primary image processing and field observations, the land cover types were defined, the training sets were identified and then the spectral patterns of land covers were generated. To classify the images, 10 training classes were used for maximum likelihood classification algorithm. Then, the classified images were assessed with the test areas and the results showed that the overall accuracy is about 93 percent. The obtained results from image processing and classification indicated the efficiency of TM data in mapping different erosion forms and land cover types. The TM thermal band (TM6) as a surrogate of surface temperature is used for displaying the variation of thermal data. The results of the application of sobel filtering in direction of northwest to the southeast have also shown the efficiency of this filter for enhancement of yardang features. From the obtained results, we concluded that the main land cover types of the yardang region could be discriminated with a high level of accuracy by supervised classification. We also generally concluded that Landsat TM thermal and TM reflective bands could be useful for studying Lut Desert conditions especially yardangs and sand dunes. We also generally concluded that hyper-arid region of Lut Desert with absence of vegetation cover, usually prevailing clear skies, a shortage of rainfall and thus low surface moisture could be considered ideal environments for remote sensing applications in the study of land cover classification.

Key words: Lut desert . yardang . thematic mapper . thermal band . classification . sand dune

INTRODUCTION

Experience has shown that some earth surface features of desert can be identified, mapped and studied on the basis of the spectral characteristics of the particular features of a Desert [4]. Therefore, a better understanding of the behavior of different regions of wavelength on surface conditions may increase the efficiency of the study of land cover types on the basis of remote sensing. The application of remote sensing in desert areas is increasing in different fields, such as mapping land cover types and terrain analysis. Most investigations have taken place in arid and semi-arid regions, because they have been considered ideal environments for remote sensing applications due to absence or near absence of vegetation cover, having usually clear skies, very low rainfall (Table 2) and thus low soil moisture conditions [17]. Landsat TM data have proved useful for mapping depositional environments on playas in Tunisia [16] and Ardakan playa in Iran [4].

Lut Desert with an area of about 80,000 Km^2 is one of the largest deserts in Iran and includes a great diversity of hydro-Aeolian processes with a very interesting pattern of yardang landforms. The Ayardang@ occupy most part of the western part of Lut Desert. Yardang is a Turkman word [10], now used in geomorphology for wind-eroded ridges of cohesive

Corresponding Author: Dr. S.K. Alavi Panah, University of Tehran, P.O. Box: 14185-354, Iran

materials [15]. The yardang is widespread in many parts of Iranian deserts. But the extent of yardang in Lut Desert is greater than in other places. Although, Lut Desert has been mapped in large scales, but no attention has been focused on the yardang land cover types. Most yardangs occur in unidirectional forms. This optimal form of yardangs minimizes the effect of wind on separation [19]. Although yardangs are formed only where fluvial action and weathering are slow, most have been initiated from forms created by non-Aeolian processes. Many have been formed out of gully terrain [19]. A number of non-Aeolian processes such as salt weathering, desiccation, cracking, slumping, piping and riling are very important in forming yardangs [8]. Although the yardangs are affected by selective wind erosion, but physiographic-geomorphologic studies show the collaborative effect of wind and water action in their formation and development. The Lut mega yardangs have recently been cut in Pleistocene lake deposits [5].

Application of remotely sensed data for geomorphologic mapping in desert regions require the knowledge of land cover types, such as desert varnish [12] and surface reflectance, in order to yield more reliable results. Information about land cover types especially eroded land, sand sheet (ERG), sand dune, salt affected land and even the air and surface conditions is required to manage deserts. To the author=s knowledge, not many researches about land cover types and surface temperatures have been published on Lut yardang landform. Kardavani (1970)[11] states that Lut Desert has one of the highest temperature zones in the world. Alavi Panah (2002,2003,2006)[1-3] stated that for a more careful and detailed interpretation of surface temperature of the study area, knowledge on landform and land cover types of yardang is helpful.

There are many approaches to map surface temperature from thermal scanner data [13]. Techniques for generating thermal maps from the TM thermal data may have the advantages of reducing cost and time in very poorly accessible regions of Lut Desert. Remote sensing has shown its greatest value where fieldwork was difficult. Therefore, in this study we applied remotely sensed data in the study of western part of Lut Desert which is poorly accessible. In fact, the main purpose of this study is to evaluate the capability of Landsat TM data for studying land cover types and geomorphology in arid conditions of Lut Desert. It seems that much of the potential future tourism development may occur in yardang region for traveling tourists to visit one of the most interesting and important eroded landform in the world such as; Yarnadgs, ERG, Aeolian form, Ripple marks that have been formed in between yardangs, One of the largest sheets that is absence of vegetation cover clear sky and etc. Therefore, the study of land cover types and surface conditions in these areas can have a practical value in the future planning and management of Lut Desert. Landsat TM data might be a useful tool to overcome the problem of non-accessibility of yardang region. To improve our understanding about one of the most interesting desert landforms Landsat TM data were used. These remotely sensed data may have the ability to differentiate the most important land cover types.

MATERIALS AND METHODS

Lut Desert is located in eastern Iran. The study area is located in the eastern part of Kerman city on the eastern part of the Shahdad town (Fig. 1). Lut Desert surrounded by the Shahkoh Mountain in the north that is located in south of Birjand and Nay Band mountain in the south, Kerman elevations in the west, Sistan elevations in the East (Fig. 1). In this study, most attention has been focused on the sub-area of LUT which covers about 120 H 60 Km (yardangs) (Fig. 2)

Figure 2 shows the study area, which is represented by two sub-areas. Lut Desert has elevations varying from 4000 m MSL in the Kerman Mountain and 56 m MSL in the yardang. The highest part of the yardang region is 399 m MSL [14] (Fig. 3 and Table 1).

In order to study the surface conditions in winter and summer, the Landsat satellite data relating to yardang areas were collected at two different dates. The only available Landsat satellite data that are used in this study area as follows:1) The total area, which is covered by Landsat TM data taken on December 5, 1998, 2) Southeast of yardang sub-area which is covered by Landsat TM, recorded on June, 24, 1989.

Table 1: Characteristics elevation classes in Yardang

Elevations classes (m)	Area (KM^2)	Percent
<200	307.5	1.3
200-220	225.5	0.9
220-240	242.8	1.0
240-260	299.5	1.2
260-280	690.5	2.8
280-300	6850.2	28.1
300-320	3748.6	15.4
320-340	1135.1	4.7
340-360	831.0	3.4
360-400	2812.9	11.5
400-450	3532.7	14.5
450-500	3690.4	15.1
Total	24366.7	100.0

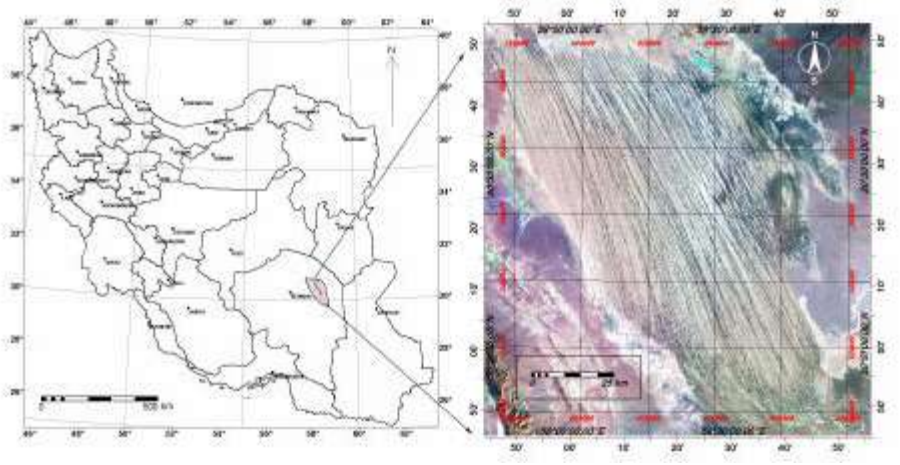

Fig. 1: Geographical location of the yardangs in Iran

Fig. 2: Geographical location of the study area: A-left figure, total yardangs area, b-right figure, south and southeast and east parts of yardangs and sand dune (ERG) area

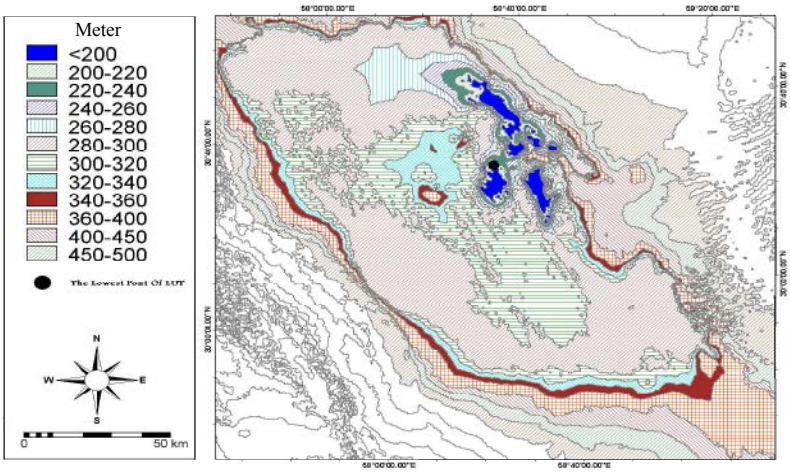

Fig. 3: Elevations classes in yardangs

Table 2: No of cloudy day (7-8)/8) and monthly total of sunshine hours and no of days with visibility less than or equal 2 km in station around lut desert

Station	Birjand			Nehbandan			Khoor biabanak			Tabass			Bafgh		
Monthly Data\month	1	2	3	4	5	6	7	8	9	10	11	12	13	14	15
Jun	5	196	2	6	212	2	6	204	0	5	202	1	6	212	1
Jul	5	195	1	5	210	1	4	215	0	4	207	1	4	220	1
Aug	7	211	1	7	226	1	7	221	0	5	231	1	7	241	1
Sep	5	236	1	3	265	1	4	256	0	4	258	1	5	267	0
Oct	2	307	0	1	320	0	2	318	0	2	319	1	2	323	0
Nov	0	337	0	0	337	0	0	338	0	0	346	1	0	355	0
Dec	0	357	1	0	363	1	0	363	0	0	356	1	0	362	1
Jan	0	355	0	0	359	0	0	358	0	0	353	1	0	366	0
Feb	0	307	0	0	318	0	0	317	0	0	317	0	0	325	1
Mar	0	288	0	0	292	0	1	296	0	0	293	0	1	302	0
Apr	2	230	0	1	250	0	2	237	0	2	232	0	3	243	0
May	4	199	1	5	217	1	4	213	0	4	201	1	5	221	0
Annual	30	219	8	28	3367	8	30	3333	3	27	3314	7	32	3437	5

1 = No. of cloudy day S (7-8)/8, 2 = Monthly total of sunshine hours, 3 = No. of days with visibility less than or equal 2 km, 4 = No. of cloudy days (7-8)/8, 5 = Monthly total of sunshine hours, 6 = No. of days with visibility less than or equal 2 km, 7 = No. of cloudy day S (7-8)/8, 8 = Monthly total of sunshine hours, 9 = No. of days with visibility less than or equal 2 km, 10 = No. of cloudy day S (7-8)/8, 11 = Monthly total of sunshine hours, 12 = No. of days with visibility less than or equal 2 km, 13 = No. of cloudy day S (7-8)/8, 14 = Monthly total of sunshine hours, 15 = No. of days with visibility less than or equal 2 km

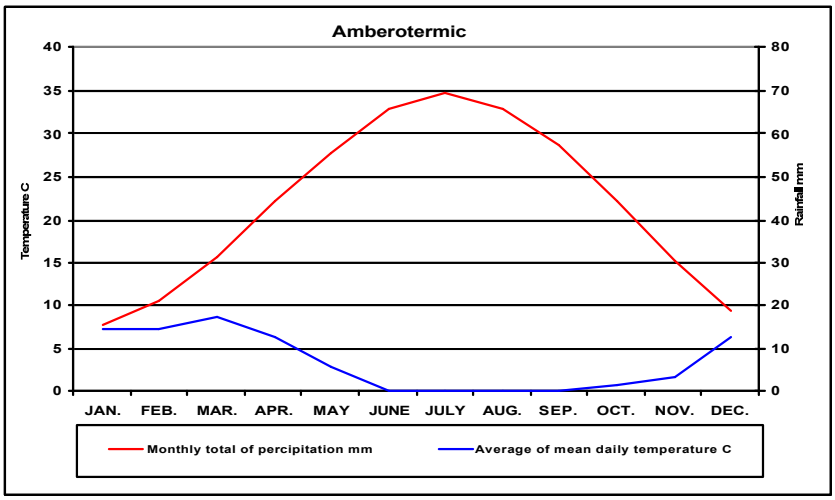

Fig. 4: Tabass amberotermic

The Lut Desert, particularly yardang regions are characterized by an extremely arid climate, with excessive summer heat and winter temperatures below freezing point and an annual rainfall less than 5o mm. Table 2 shows clear sky and monthly total of sunshine hour and no of days with visibility less than or equal to 2 km in station around Lut desert. Figure 4 illustrates the Amberotermic Curve of the Tabass area near Lut area with hyper-aridity.

The hyper-arid southeast of yardang region consists of large gravel plain and desert pavement, sand dunes and salts lands. The sand areas (LUT ERG) in the east of yardang form the largest body of sand in Iran. This area is covered with longitudinal crescent dunes (Fig. 7and 8).

Data acquisition and processing: To perform this study, we used seven bands of TM Landsat 5, taken on December 5, 1998 and June 24, 1989. From the full image, a window of yardang region (Fig. 2a) and a window of southeast of yardang region (Fig. 2b) were selected. In this study, we hypothesized that Landsat

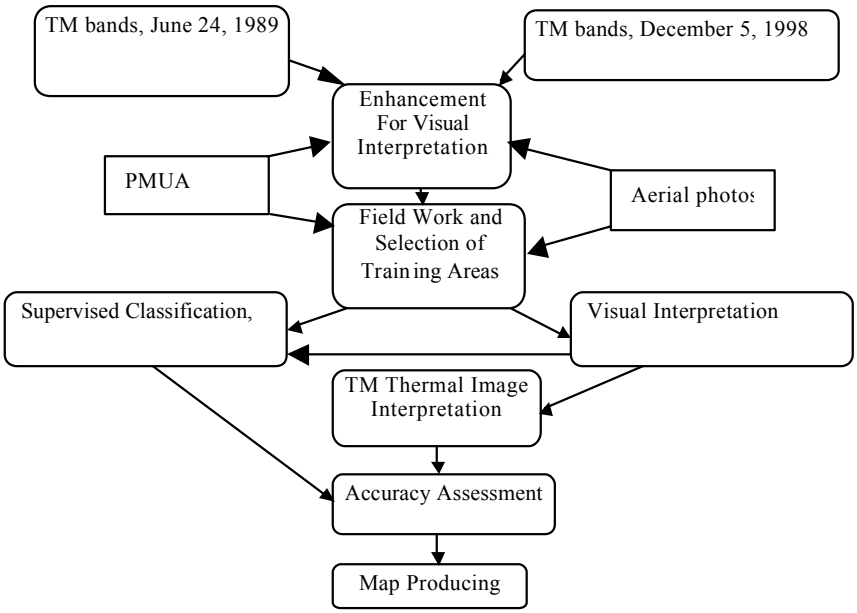

Fig. 5: Flowchart showing the methodology of the study

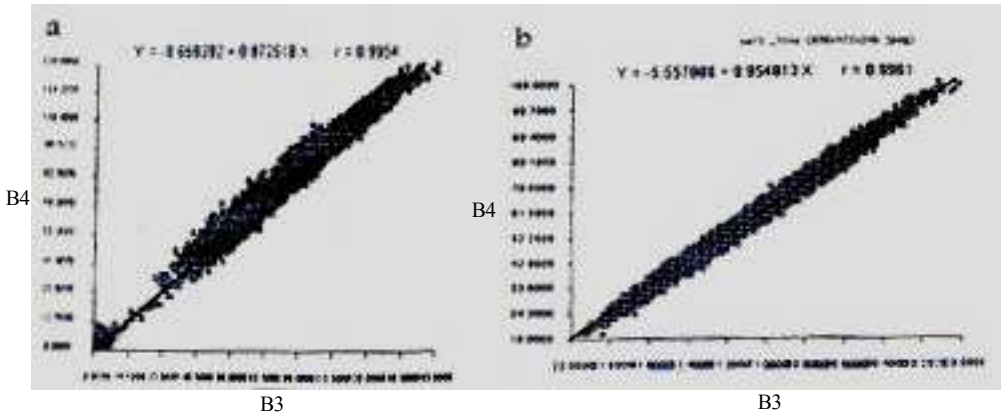

Fig. 5: Soil lines obtained from the plot between TM3 and TM4 four: a) June, 1989 and b) December, 1998

TM data with spatial resolution of 30m for reflective bands and 120 m for thermal band are useful for the study of land cover types and surface conditions. In this research, the methodology was comprised of; 1) primary image processing and field work 2) image processing, 3) two dimensional Feature Space (FS) analysis and 4) image classification and accuracy assessment.

In this study, the three-band combinations were ranked based on Optimum Index Factor (OIF) [6] and the different False Color Composites (FCC=s) were created. The different combinations of three bands, such as false color image utilizing TM bands 7 in red, 4 in green and 1 in blue were evaluated visually based on the obtained information from field work and image interpretation criteria.

The thermal map was produced using TM6 and level slicing in order to show discrete thermal range as a surrogate of temperature range.

A Principle Component Analysis (PCA) was performed based on the correlation matrix. PCA is applied to 7 TM bands (including TM thermal band with the same pixel size of TM reflective band of 30m in order to compress multi-channel data and to condense the original data into a new set of variables which are called PC's. The TM6 data as a representative of surface temperature is used to display the variation of thermal data. This study was performed using Landsat TM data and other information sources, such as topographic maps (1:50,000), geologic maps (1:250,000)) and aerial photos (1:20,000).

Field work: The field work as one of the most important steps was carried out in autumn season of 2000 to confirm the nature of findings (Fig. 5). Based on field observations, the land cover types were defined and the training sets were identified and spectral patterns of different types of land covers were generated. Based on the obtained results from OIF, TM bands 1, 4, 5, 7 as the most informative TM reflective bands were used to classify land cover types using a per pixel maximum likelihood classification algorithm (Fig. 5). To enhance the images, stretching and filtering techniques were used. Based on the obtained results, 10 different classes were distinguished of which five classes are related to yardang.

RESULTS AND DISCUSSION

Soil line: Table 3 shows the correlation coefficients between TM bands, a) dated June 1989 and b) December, 1998. The highest correlation coefficients were found between the TM3 and TM4, which forms a soil line.

Table 3: Correlation matrix of TM bands dated: a) June 1989 and b) December, 1998 of southeast of Lut Desert

	TM1	TM2	TM3	TM4	TM5	TM6	TM7
a							
TM1	1						
TM2	0.983	1					
TM3	0.948	0.982	1				
TM4	0.913	0.961	0.996	1			
TM5	0.852	0.917	0.948	0.961	1		
TM6	-0.561	-0.577	-0.548	-0.531	-0.566	1	
TM7	0.821	0.892	0.931	0.951	0.991	-0.531	1
b							
TM1	1						
TM2	0.971	1					
TM3	0.961	0.985	1				
TM4	0.965	0.982	0.995	1			
TM5	0.921	0.954	0.963	0.964	1		
TM6	-0.401	-0.415	-0.406	-0.4o1	-0.396	1	
TM7	0.917	0.951	0.963	0.965	0.988	-0.378	1

Table 4: The rank of 35 possible band combinations of the TM bands based on their OIF values

	Band combination	OIF value	Rank	Band combination	OIF value
1	1/5/2006	24.12	18	1/4/2007	17.87
2	1/6/2007	21.60	19	1/3/2005	17.79
3	3/5/2006	21.50	20	1/2/2006	17.73
4	5/6/2007	21.25	21	4/5/2007	17.59
5	4/5/2006	21.09	22	2/3/2005	17.32
6	1/5/2007	20.80	23	2/5/2007	17.28
7	1/3/2006	20.53	24	2/6/2007	17.14
8	1/4/2006	20.09	25	1/3/2004	17.13
9	1/4/2005	19.96	26	1/2/2007	16.81
10	2/5/2006	19.76	27	2/3/2006	16.70
11	3/6/2007	19.33	28	2/4/2005	16.69
12	1/2/2005	18.79	29	2/4/2006	16.07
13	1/3/2007	18.48	30	1/2/2003	15.86
14	3/5/2007	18.46	31	3/4/2007	15.84
15	4/6/2007	18.34	32	1/2/2004	15.50
16	3/4/2006	18.28	33	2/3/2007	15.28
17	3/4/2005	17.92	34	2/4/2007	14.61
			35	2/3/2004	14.26

Due to lack of vegetation (zero vegetation cover) in the study area, the strong relationships between TM3 and TM4 have very high correlation coefficients of 0.995 and 0.996 for dates of December 5, 1998 and June 24, 1989 respectively. The obtained results from high correlation coefficients between TM3 and TM4 reveals lack of vegetation that normally exhibits low reflectance in near infrared band and high reflectance in the red band (Fig. 5). Thus, the FS between TM red and TM infrared makes a soil line and it does not produces a triangular shaped region. The position of spectral measure on both soil lines (Fig. 5a and 5b) confirms the lack of vegetation in the study area. The obtained results from soil line confirm what was stated by Kardavani (1970)[11]. They argued Lut Desert is free of vegetation.

Image enhancement and color composites: In order to select the most suitable three band combinations for creating color composite, the Optimum Index Factor (0IF) criteria was applied to 7 TM bands. Based on the results obtained from OIF, the TM reflective and thermal band combinations 6, 5 and 1 ranks first in terms of the 0IF values (Table 4). The three band combinations with the highest OIF values generally will have the most information (as measured by variance) with the least amount of duplication (as measured by correlation). Application of the OIF criteria to seven TM resulted in 35 combinations. It is evident from the Table 4, that the band combination 1, 5, 6 ranks first in terms of OIF values. Therefore, we may conclude that the maximum information is provided by the first three ranks. Interestingly the TM thermal band is in the first

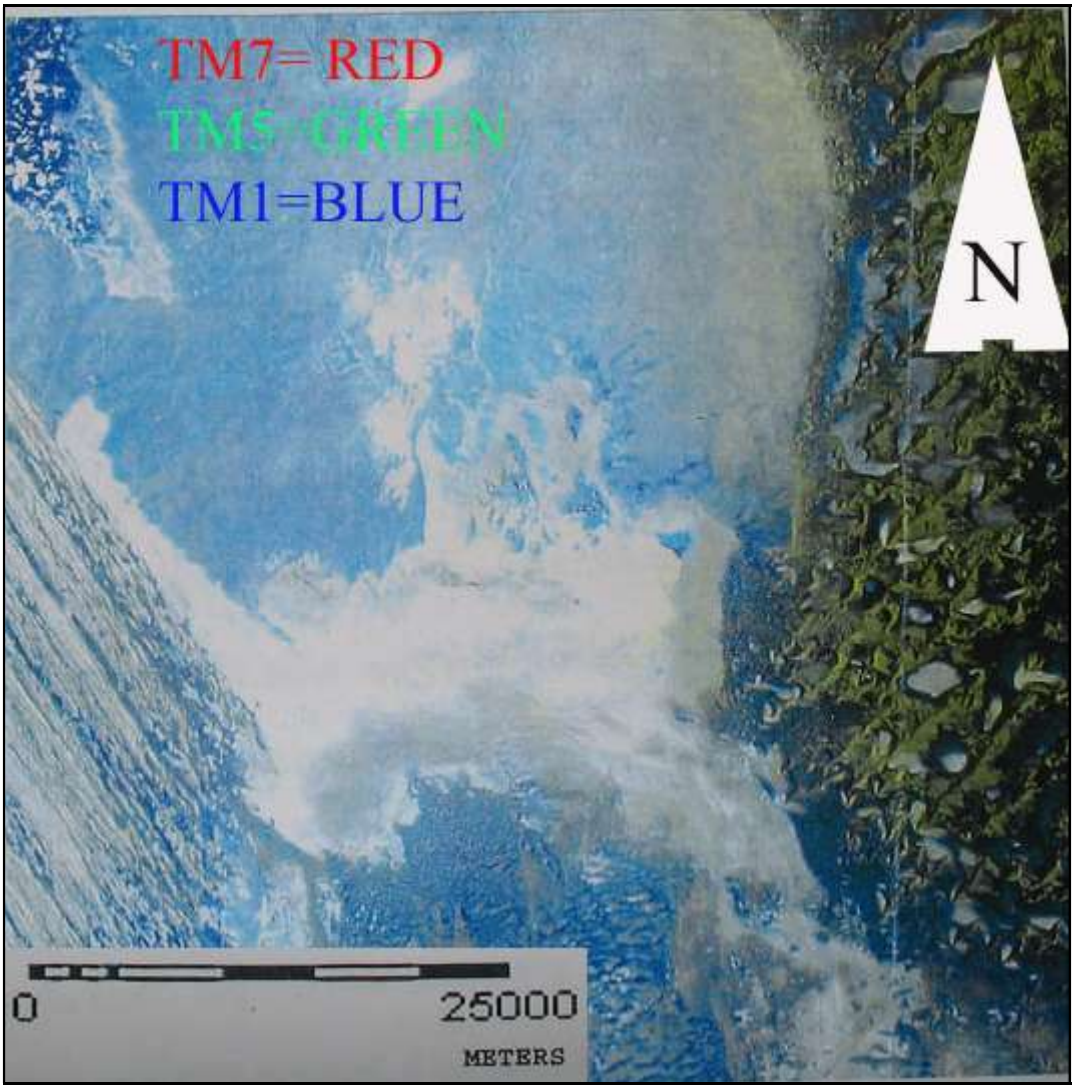

Fig. 6: Color composite of landsat TM over southeast of yardang region that uses TM band 7 in red, band 5 in green and band 1 in blue

Table 5: Eigenvectors of the seven components of the whole TM scene of yardang

	TM1	TM2	TM3	TM4	TM5	TM6	TM7	Variance (%)
PC1	0.397	0.413	0.415	0.411	0.398	0.102	0.403	79.63
PC2	-0.075	0.019	0.051	0.084	0.091	-0.985	0.076	14.89
PC3	-0.536	-0.313	-0.182	-0.048	0.569	0.111	0.494	3.76
PC4	-0.557	-0.057	0.375	0.645	-0.258	-0.080	0.183	1.04
PC5	-0.325	-0.511	-0.092	-0.343	-0.481	-0.006	0.525	0.31
PC6	0. 330	-0.080	0.165	-0.414	-0.020	-0.513	0.070	0.25
PC7	0.047	0.356	-0.798	0.510	-0.138	-0.001	0.128	0.14

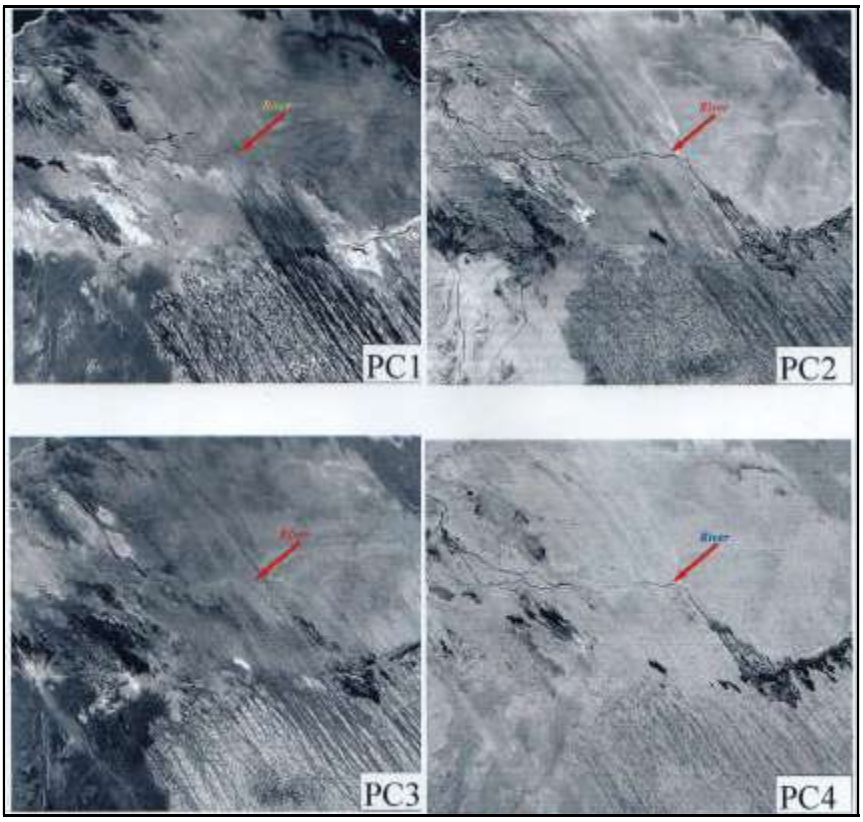

Fig. 7: Comparison between the four PCs reveals that the main rivers are visible on all 4 PCs but the minor rivers, surface gullies and surface conditions are only visible on PC2

15 ranks (ranks 1 to 15). This means that TM thermal band contains much information about the study area.

In this study, the color composites were created and they were displayed on monitor and they were compared with regard to discrimination among the land cover types. The obtained results have shown that FCC 7-5-1 exhibits wet land, sand dune and sand sheet better than other color composite images. The regions rich in sand sheets, exhibit yellow color and wet land regions appear in blue color (Fig. 6).

In this study, the PCA transformation was applied to 7 Landsat TM bands based on the correlation matrix and the result is shown in Table 5.

Table 5, shows the eigenvectors computed from the correlation matrix. The first principal component of the TM scene accounts for 79.63% of the total variance. PC2 accounts for 14.89% of the total variance. PC3 accounts for another 3.76% bringing the total variance to 98.28%, which is explained by the first three PCs. Thus, 7 TM data set were compressed into just three PCs that describe about 98% of the total variance. The remaining PCs (PC4, PC5, PC6 and PC7) accounts for about 1.7 percent of variance. The result of the PCA shows that TM bands 1, 2, 3, 4, 5 and 7 with the highest eigenvector are highly related to PC1 while TM thermal band with the highest eigenvector (-0.985) is heavily

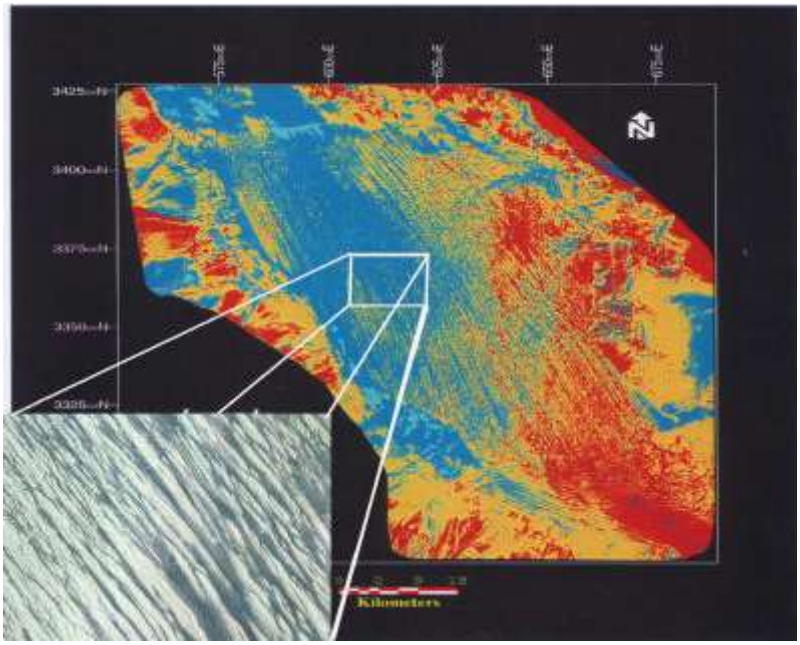

Fig. 8: The results of the application of sobel filter in direction of northwest to southeast of yardang

attributed to PC2. The PC2 largely depends on the TM thermal band and weakly attributed to TM reflective bands and therefore PC2 may be labeled as temperature and/or moisture component.

The obtained results from PCA have shown that PC2 contain a great deal of useful information especially about the rivers and wet land areas (Fig. 7).

From the above results, we may conclude that PC1 and PC2 contain a lot of information on surface conditions and surface temperature respectively. Comparison between the four PCs reveals that the main rivers are visible on all 4 PCs but the minor rivers; surface gullies and surface conditions are only visible on PC2 which greatly contributes to TM6 (Fig. 7).

The results of the application of sobel filtering in the direction of northwest to southeast have also shown the efficiency of this type of filter for a better enhancement of yardang features such as ridges, furrows and even eroded gullies (Fig. 8). Figure 8 shows the ridges and corridors of the landform. The signs of water erosion can bee seen in the form of rill erosion. The corridors, which were located between the ridges, consist of ripple mark landforms or sand dunes. Geomorphologic studies of ridges and corridors indicate that the dominant direction of the wind in the area is northwest to southeast.

Variation of thermal values: The TM band 6 data of the yardang region shows that the data are in a narrow range of 69 to 176 in a total range of zero to 255. Figure 9 shows the stretched TM thermal image of yardang with 7 transects on it. TM 6 DN values along 6 transact (lines 1 to 6) suggest that a zone of relatively higher thermal values could be delineated in the eastern part of yardang when compared with the values present in the western part. This difference in thermal values (as a surrogate of surface temperature) suggests that this kind of lineament has acted as a thermally different zone divider. These observed thermally different zones may be related to the fault impact. To find an explanation about the correlation between lineament and thermal zones in the eastern and western margins of Lut Desert, further research is needed. Line 7 in Fig. 9, shows the trend of thermal DN values from northeast to southwest. Figure 9 shows the transect 1 to 6 with various peaks and valleys which may correspond to the ridges and furrows with different surface materials, topographic conditions, shadows and sunlight illumination.

The peak with the highest TM DN values is mainly associated with sun-exposed ridges, sand sheet or sand dunes. The valleys correspond to shadows and other phenomena. The transect 4 shows that a deep valley exists near the endpoint of line 4 which represents the wet zone. Figure 10 shows the thermal image with 5 discrete classes of: 1) very high, 2) high, 3) moderate 4) low 5) very low. The arrows indicate two different thermal zones in eastern and western part of lineament.

Field work and representative training sites: The field work as one of the most important steps was carried out in October, 2000. The aim of this study is to

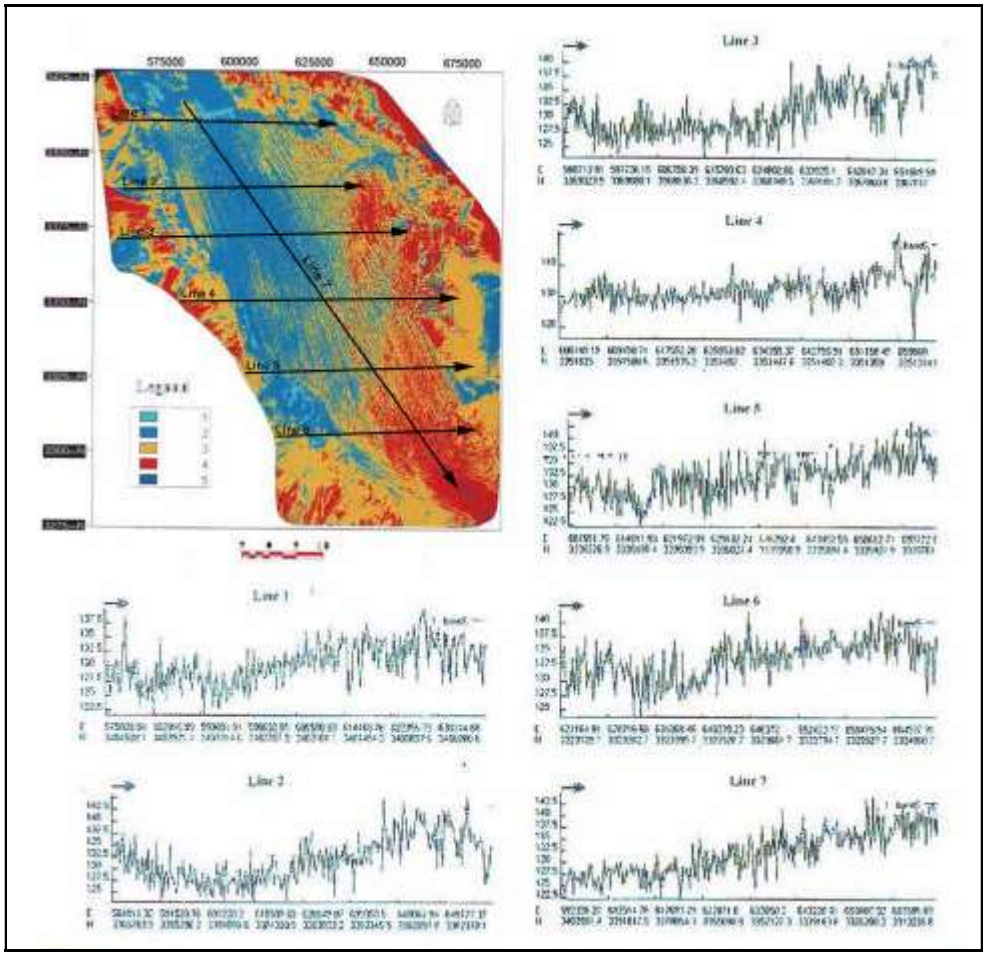

Fig. 9: Shows the thermal DN value information along 6 specified transects from west to east (lines 1 to 6) and line 7 show the thermal DN values from northwest to southeast

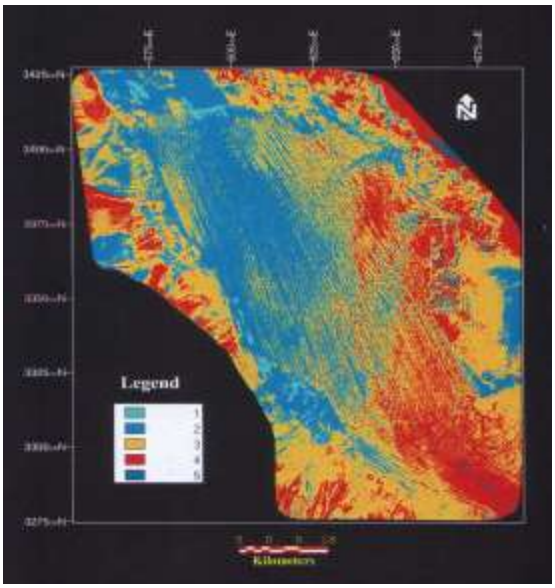

Fig. 10: Shows the thermal image with 5 discrete classes of thermal data: 1) very high, 2) high, 3) moderate, 4) low 5) and very low. The arrows indicate two different thermal zones in eastern and western part of the lineament

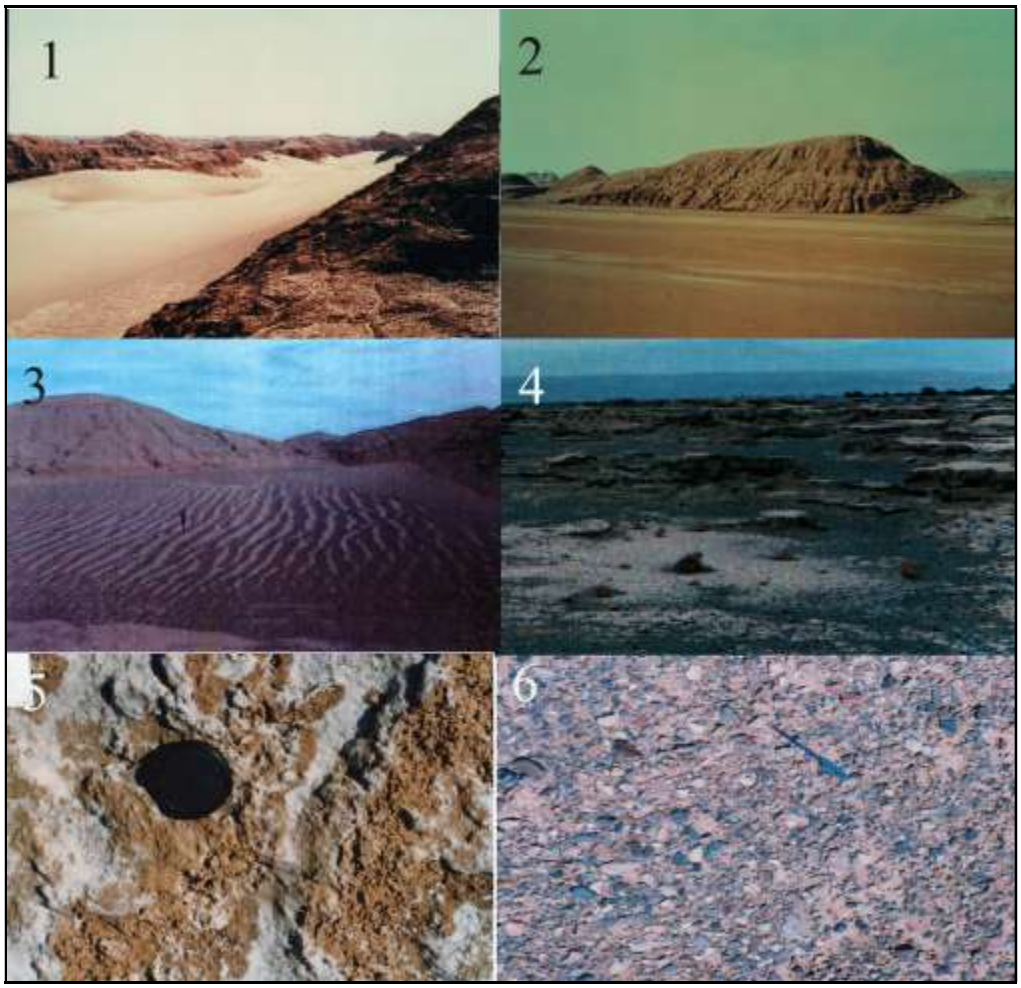

Fig. 11: Surface conditions of training classes: 1) sand dune between yardang ridges, 2) yardang ridges, 3) sand sheet, 4) salty land 1, 5) salty land 2, 6) desert pavement

identify and to map land cover types and their corresponding geomorphologic features. Visual image interpretation was used to identify the land cover types of the area. The standard TM FCC at the scale of 1:100,000 and aerial photos at the scales of 1:50,000 and 1: 20,000 were the main images and maps, which were used in the field. Some other maps, such as topographic and geologic maps were used during the fieldwork for delineating the boundaries of the morphologic units and land cover types.

As a result, the classes of Yardang (Y), Desert Pavement (DP), Sand Dune (SD), great sand dunes (Erg1 and Erg2), Salty Land (SL1 and SL2) and Wet Land (W1 and W2) were trained. The training classes: 1) sand dune between yardang ridges, 2) yardang ridges, 3) sand sheet, 4) salty land1, 5) salty land 2, 6) desert pavement.

Decisions about where to take samples are of great importance, since the validity of extrapolations about the whole target area is highly dependent upon the design of the sampling scheme [18]. Purposive samplings were done where the typical sites are chosen for a special goal. Proponents of purposive sampling argue that the resultant samples are very representative since they are based on the skills and the local knowledge of the field worker. The execution of the fieldwork was based on the more recent TM FCC that is simplified and guided by TM PMU maps. TM FCC and associated TM PMU and other ancillary data and information, such as soil salinity, geologic and eroded maps plus explanatory reports were used. Based on the results obtained from the fieldwork and the information obtained from the maps (1:50,000), aerial photos (1:20,000), geologic maps and our 20-year-personal experience in the Iranian Desert, the training areas were chosen to classify the TM images. Ancillary data, image interpretation in a visual way and PMUA were used to improve the classification accuracy. The

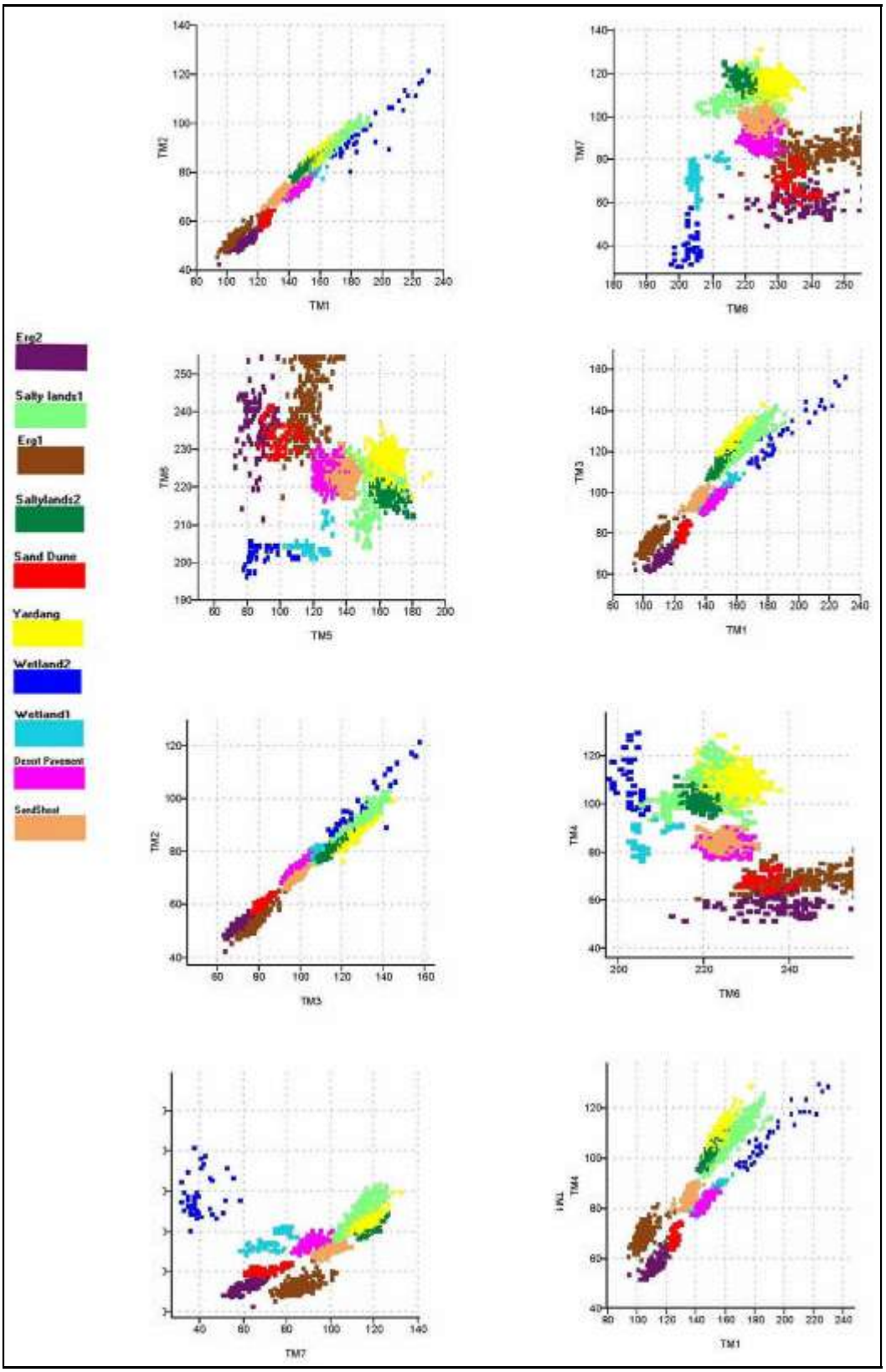

Fig. 12: The feature space between TM 1, 2, 3, 4, 5, 6 and 7

advantage of PMUA is that it can be adapted to all possible photographic scales and landscapes [9].

This method was used for aerial photographs or satellite images. In this study, the main purpose of the PMUA is to make the sampling easy and to organize the fieldwork and to select the location of samples. Based on the obtained results from hypsometric (the measurements of heights as with reference to sea level) studies, fieldwork, false color composites and topographic maps, the greatest ridges of yardangs have a length of 600 m, a width of 140 m and a height of 30 m while the smallest yardangs have a length of 50 m, a width of 30 m and a height of 20 m.

Sampling and spectral separability: Several researchers have indicated that a minimum 50 of samples of each land cover type has to be included in the error matrix [13]. If the area is large and the classification has a large number of land cover types, the number of samples in each category should be increased to 75 or 100 [7]. Therefore we attempted to optimize the number and strategy of the sample points in the withheld test areas. Due to the fact that for the classification accuracy, the information used must be very reliable, therefore a limited number of samples were possible to be selected in the study area. Due to this limitation, the minimum 52 (class no. 5) and the maximum 317 (class no. 2) pixels in different areas and many places were selected randomly.

The validity of training data was evaluated from visual examination of FS and quantitative characterization, such as the mean and standard deviation (SD) of the training classes. Among the 10 training classes, the class no. 10 (wet land) shows the highest SD for TM 7 that is due to heterogeneity of soil surface moisture, salinity and lithology variations.

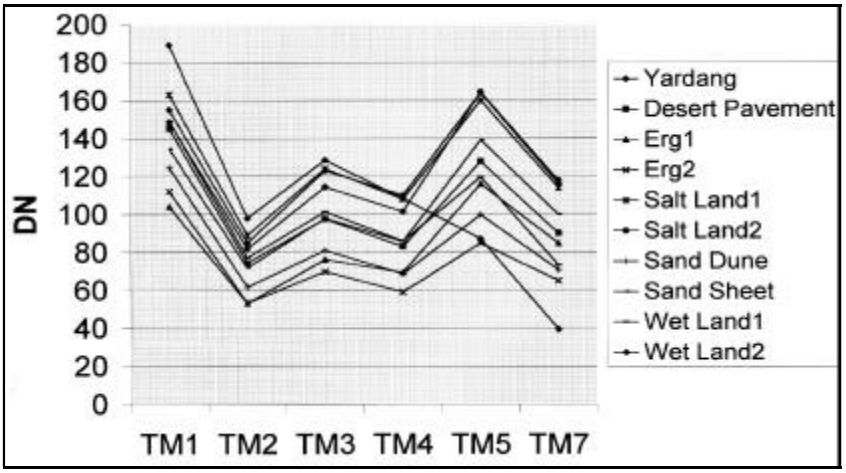

Fig. 13: Shows plot of the mean of training classes over TM bands

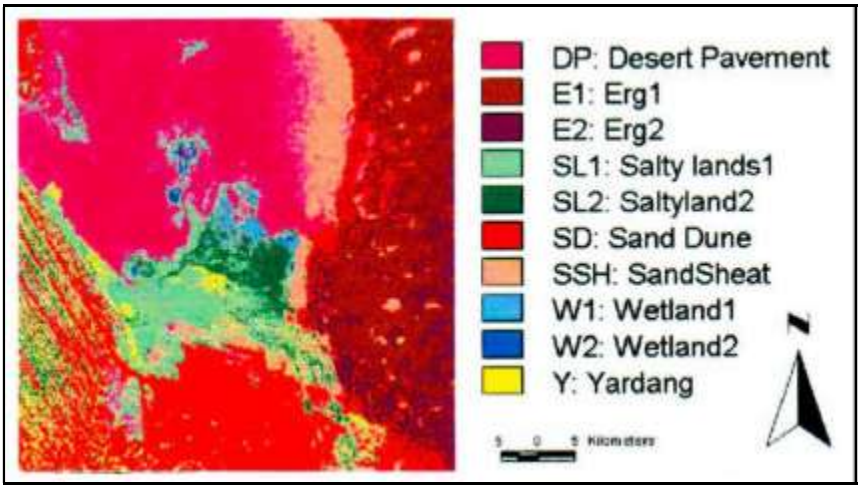

Fig. 14: Land cover classification image of southeast of yardang region based on maximum likelihood classification algorithm

Spectral separability helps refining the digital classification and it has been used as an index of the efficiency of sensor data to distinguish various terrain features and phenomena. Figure 12 and 13 show the FS between TM band1, 2, 3, 4, 5, 6 and 7. A close look at this FS indicates that the behavior of TM bands is different in viewpoint of spectral separability. For example, FS bands 4 and 7 indicates a fairly good spectral separability of training classes, while the FS bands 3 and 4 (soil line) shows mixing between the training classes.

It means that the overall separability of classes is poor in TM2 and TM4 data set. Figure 13, shows the plot of the mean of training classes over TM bands. This figure reveals the role of different bands especially TM bands 7, 5 and 1 in separability of the classes. The salty land of the study area shows a large diversity in surface characteristics. A different portion of white and gray brown to brownish color of salt crust and salty land varies from field to field. Surface roughness of the salty land can be also an important factor in its heterogeneity.

It should be noted that due to great differences in the soil surface characteristics of the salty land, two classes of salty lands were necessary to be trained. The salty land 1 (no. 2) is completely different from salt crust class (no. 4) in terms of surface and also subsurface characteristics (Fig. 11-13).

Image classification and accuracy assessment: The training samples, which are used to estimate the statistical characteristics of the classes, were used to classify the TM scene. The results of maximum likelihood classification of the selected TM bands 7, 5, 4 and 1 of southeast part of yardang area are shown in Fig. 14.

A one to one comparison was made between the ground truth data and the information available in reports, fieldwork and maps (Table 6). In fact, other areas of representative land cover types (test areas), different from training samples were used to assess the accuracy of the classified image. The areas which were withheld for the assessment of the classified image are called test areas. An accuracy estimate in terms of overall accuracy was made after generating confusion matrix. The training area accuracy however indicates little about performance of the classifier in other areas (Non-trained areas) in the scene. Therefore, other areas of representative land cover types (test areas), different from training samples were used to assess the accuracy of the classified image.

The height average of Yrdangs classes is lowest in Lut desert (Fig. 16). Figure 17 shows some statistical parameters of geomorphology classes of Yardangs in Lut desert.

For generating confusion matrix the test site pixels were crossed with the classified image and tabulated in

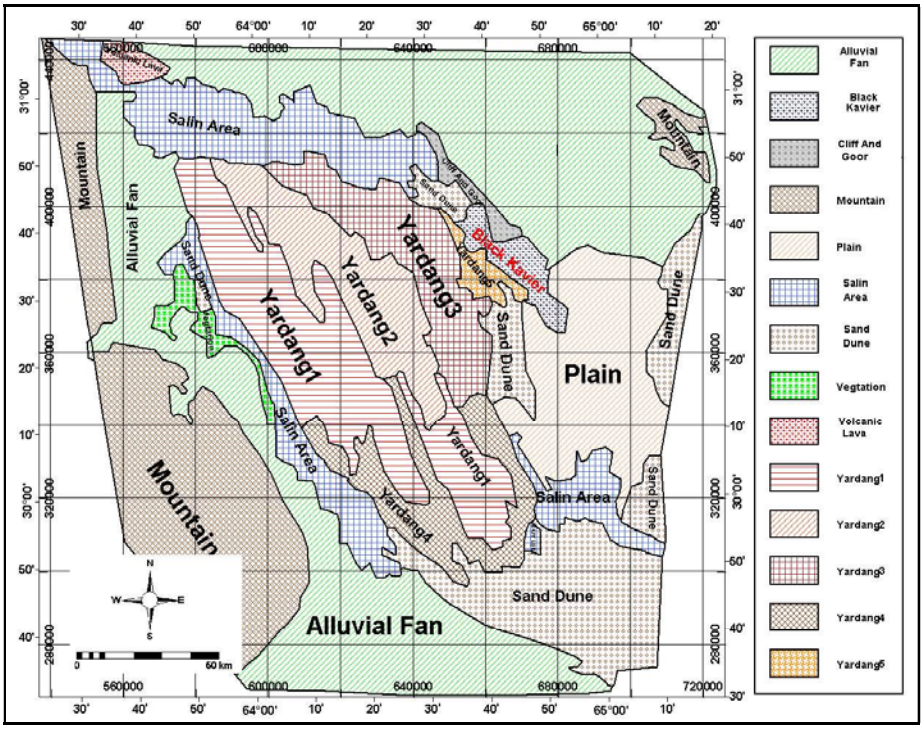

Fig. 15: Classes of yardangs

Table 6: Error matrix resulting from maximum likelihood classification using TM bands 1, 4, 5 and 7

No.		Y	SL1	DP	SL2	W1	SSH	E1	SD	E2	W2	Total	Accu.
1	Y	108	17		2							127	85.04
2	SL1	57	254	1	4				1			317	80.13
3	DP			167			1		4			172	97.9
4	SL2	1			217							218	99.54
5	W1					46			2		4	52	88.46
6	SSH						197		9			206	95.63
7	E1							176		1		177	99.44
8	SD	7							226	15		248	91.13
9	E2					1	1	1		224		227	96.68
10	W2						1		1	61		63	96.83
Total		173	271	168	223	47	200	177	243	240	65	1807	93.20
*Accu		64.43	93.73	99.40	97.31	97.87	98.50	99.46	93.00	93.33	93.85	92.89	

*Accu = Accuracy

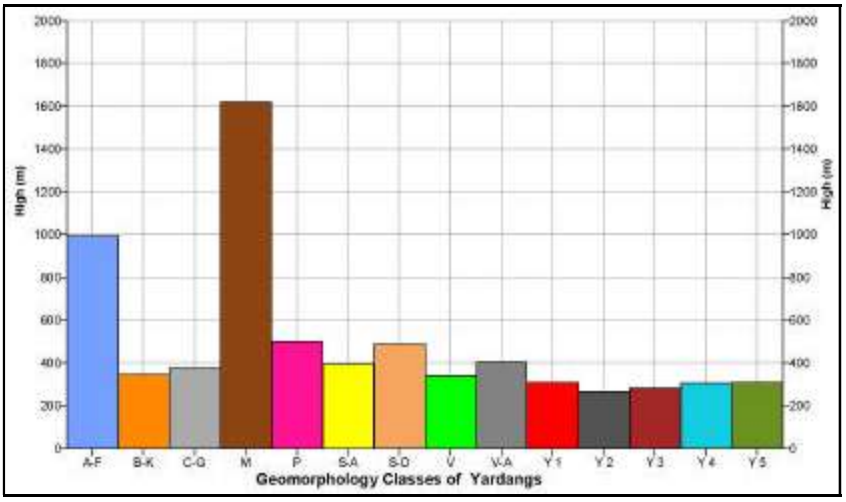

Fig. 16: The height average of geomorphology classes in Lut desert

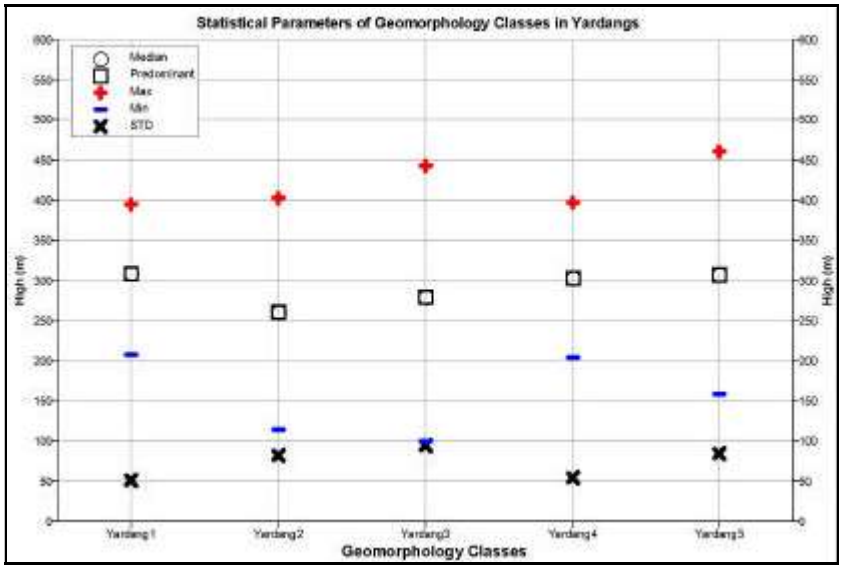

Fig. 17: Statistical parameters of geomorphology classes in yardangs

a contingency table (Table 6). In this contingency table, the accuracy per category and the overall accuracy were computed in the same way as training areas. The computed overall accuracy is 91.3%. Although the overall classification accuracy based on the test area is high, but a detailed interpretation and inspection of the error matrix is necessary to appreciate each of the land cover types.

For example, some classes such as SL2 class (no. 4) with 99.54% accuracy are more reliable than some other classes such as SL1 class (no. 2) with classification accuracy of 82%. Due to similar spectral characteristics, these two classes of SL1 and yardang can not be discriminated with a very high accuracy, but the separation of these two classes might be possible by using ancillary data such as Digital Elevation Model.

CONCLUSION

This study has demonstrated the utility of TM data for mapping Lut Desert features including yardang, sand dune and some other land cover types with relatively high spatial resolution satellite data. We concluded that Lut Desert land cover types, such as yardang, sand dune and salty lands carry unique and important information about the desert characteristics. This study also showed that, in some cases, only slight spectral difference could be used effectively in discrimination of desert land cover types based on their spectral signatures. Based on obtained results from field observations we may generally conclude that non-Aeolian processes such as cracking, piping, riling and salt weathering are very important in developing and forming yardangs. To achieve high classification accuracy, extensive fieldwork and aerial photos are very effective. The result of visual interpretation of various band combinations may improve our knowledge of the spectral reflectance of wet land, sand dune and yardang and therefore, it may provide an opportunity for delineating land cover units. Based on the results obtained from FS analysis we may conclude that hyper-arid climatic conditions are ideal conditions for mapping detailed land cover types and understanding the behavior of TM thermal and TM reflective bands. The obtained results from fieldwork have revealed that wind and water do not work in isolation; quite on the contrary, they work in close partnership. Further researches seem to be necessary for improving our knowledge about mapping surface temperatures based on satellite thermal data. We may also conclude that Landsat data can be applied for mapping yardang land cover types. The digital images are available with worldwide coverage for different seasons and over a period of many years. Global availability of aerial photographs is limited therefore such availability of satellite data allows the images to be selected at optimal times for land cover change detection.

ACKNOWLEDGMENTS

The current research presented in this paper, was done in the framework of the project which was supported by the vice chancellor for research, University of Tehran. We would like to express our thanks to the Iranian remote sensing center for providing Landsat TM data.

REFERENCES

1. Alavi Panah, S.K., 2006. Thermal remote sensing and its application in the earth sciences. Universaity of Tehran Press, pp: 523.
2. Alavi Panah, S.K., 2003. Study of surface temperature Lut Desert based upon Landsat thermal band and field measurement Biaban, 7: 67-79.
3. Alavi Panah, S.K., M.R. Sarajian and Ch.B. Komaki, 2002. Temperature map of Lut Desert using thermal band of Landsat satellite. Biaban, 7: 85-99.
4. Alavi Panah, S.K., 1997. Study of soil salinity in the Ardakan area, Iran, based upon field observations, remote sensing and a GIS, Gent, University of Gent Ph.D Thesis, pp: 292.
5. Bobek, H., 1969. Zur Kennis der sudlichen Lut. Mittlungen der Ostereicher geograpischen Gesselschaft, Wein, 3: 155-192.
6. Chavez, P.S.J., C. Guptill and J.A. Bowel, 1984. Image processing techniques for thematic mapper data. In: Proc. Am. Soc. Photogrametry Conf., Washington, 728: 752.
7. Congallton, R.G., 1991. A review of assessing the accuracy of classification of sensing of environment, 37: 35-46.
8. Cooke, R.U., A. Warren and A.S. Goudie, 1993. Desert Geomorphology (London: University College London Limitted Press).
9. Daels, I. and M. Antrop, 1977. The extraction of soil information from remote sensing documents. Penol., 27: 123-190.
10. Heiden, S., 1903. Central Asia and Tibet. New York: Scribners, Vol: 2.
11. Kardavani, P., 1970. Some soil samples of Shahdad area (Kerman) No. 5. Institute of Geography, University of Tehran.
12. Keneam, N.H., 2001. Influence of Desert varnish on the reflectance of gossans in the context of Landsat TM data, Southern Red Sea Hillsm Sudan. IN. J. Remote Sensing, 2: 1869-1888.

13. Lillesand, T.M. and R.W. Kiefer, 1994. Remote sensing and image interpretation (4th Edn.). New York, John Wiley and Sons.
14. Mashhadi, N.S.K., Alavi Panah and Ahmadi, 2003. Geomorphology studies of Lut Yardang. Biaban, 7: 25-43.
15. Mc Cauley, J.F., M.J. Grolier and C.S. Breed, 1970. Yardangs of Peru and other desert regions. USGS Interagency Report, Astrogeol., Vol: 81.
16. Millington, A.C. *et al*., 1989. Monitoring salt playa dynamic using thematic mapper data. IEEE Trans. Geosci. Remote Sensing, 27: 745-761.
17. Mulder, M., 1987. Remote sensing in soil science. Development in Soil Science, Elsevier. Amsterdam, the Netherlands, pp: 379.
18. Townshend, R.G., 1981. Terrain analysis and remote sensing, London: George Allen and Unwin, pp: 232.
19. Ward, A.W. and Greeley, 1984. Evaluation of the Yardangs at Rogers Lake California. Geol. Soc. Am., Bulletin, 95: 829-837.